PROCEEDINGS OF SCIENCE

Further development of a Lamb-shift polarimeter

N. Faatz,[a,b,c,*] **B. Breitkreutz,**[a] **R. Engels,**[b] **R. Gebel,**[a,b] **K. Grigoryev,**[a] **C. Kannis,**[d] **S. Pütz,**[a,e] **H. Soltner**[f] **and Y. Valdau**[a]

[a] *GSI Helmholtzzentrum für Schwerionenforschung GmbH, Planckstraße 1, 64291 Darmstadt, Germany*

[b] *Institut für Kernphysik (IKP-2) Forschungszentrum Jülich, Wilhelm-Johnen-Straße 1, 52428 Jülich, Germany*

[c] *III. Physikalisches Institute B, Rheinisch-Westfälische Technische Hochschule Aachen, Templergraben 55, 52062 Aachen, Germany*

[d] *Institut für Laser- und Plasmaphysik, Heinrich-Heine-Universität, Universitätstraße 1, 40225 Düsseldorf, Germany*

[e] *Institut für Kernphysik, Universität zu Köln, Zülpicher Straße 77, 50937 Köln, Germany*

[f] *Zentralinstitut für Engineering, Elektronik und Analytik (ZEA) Forschungszentrum Jülich, Wilhelm-Johnen-Straße 1, 52428 Jülich, Germany*

E-mail: n.faatz@gsi.de, r.w.engels@fz-juelich.de

The Lamb-shift polarimeter (LSP) is a useful detection apparatus to verify nuclear spin polarization for atoms, molecules and ions consisting of hydrogen and/or its isotopes. Its functionality relies on the creation of metastable hydrogen atoms via a charge exchange reaction that preserves the nuclear polarization in a strong magnetic field. The nuclear polarization is then determined by analyzing the relative occupation numbers between different metastable hyperfine states with different nuclear spin projection m_I. This makes the LSP a very rapid and cost efficient detection method for beams with a beam energy in the keV range as no pre-acceleration is needed. In the past it was shown that many of the above mentioned candidates like H^+, D^+, HD etc. could be measured with success, and in this work an additional ion, i.e. H^-, adds up to the list. Furthermore, the measurements of polarized H^- ions have been performed for pulsed beams as it was in use for long times at the cooler synchrotron COSY in Jülich. In the second part, a theoretical outlook for possible adaptations to the spin filter is given, which is an important component of the LSP. This paves the way to realize experiments investigating the bound beta decay or parity violation in metastable hydrogen atoms. In addition, a short outlook for possible applications of ^3He beams is given.

20th International Workshop on Polarized Sources, Targets, and Polarimetry (PSTP2024)
22-27 September, 2024
Jefferson Lab, Newport News, VA

*Speaker

PoS(PSTP2024)011

1. Introduction

The Lamb-shift polarimeter was developed in the middle of the 1960's to measure the nuclear polarization of keV beams of atoms, molecules and ions composed of hydrogen and its isotopes [1]. Due to charge exchange reactions metastable hydrogen atoms in the $2S_{1/2}$ set are produced and subsequently the famous Lamb-shift [2] between the long-lived metastable set [3] and the short-lived excited $2P_{1/2}$ hydrogen states [4] is utilized. The so-called spin filter [5, 6] takes advantage of the Lamb-shift [2] permitting it to quench all metastable hyperfine states except for one into the groundstate. By varying between two dedicated operation modes, states with different magnetic nuclear spin projection m_I are selected. Subsequently, the Stark effect [7] is used in the quenching chamber to also bring the last metastable hydrogen atoms in a single hyperfine state into the ground state, while the produced Ly-α photons, detected by a photomultiplier [8], produce a signal equal to the relative occupation numbers of the remaining metastable atoms. As the detection process takes a short amount of time a "live analysis" of the nuclear polarization of sources and internal gas targets is possible. In addition, the running cost of the Lamb-shift polarimeter is rather low as no pre-acceleration of the beam is needed. This is the reason for its appearance at different experiments around all over the world, e.g. at the internal ANKE target at the cooler synchrotron COSY in Jülich [9].
Moreover, new developments make the Lamb-shift polarimeter suitable for different experiments addressing physical processes involving the detection of metastable hydrogen atoms, e.g. the bound beta decay [10] or the parity violation experiments in metastable hydrogen [11].

2. Hyperfine states in external fields

Hyperfine states are often represented in two different bases, the coupled $|F, m_F\rangle$ and the uncoupled representation $|m_J, m_I\rangle$. Its importance is explained by taking an external homogeneous magnetic field $\vec{B} = B_0\hat{e}_z$ into account. The corresponding Hamiltonian describing the dynamics is given by

$$H_{BR} = A\frac{\vec{I}\cdot\vec{J}}{\hbar^2} + \left(g_j\mu_B\frac{\vec{J}}{\hbar} - g_p\mu_k\frac{\vec{I}}{\hbar}\right)\cdot\vec{B}, \tag{1}$$

where the first term describes the hyperfine interaction by a magnetic dipole interaction and the second term gives the interaction of the spins of the atom with the external magnetic field [12, 13]. Moreover, A stands for the hyperfine constant while g_j describes the Landé g-factor and g_p the nuclear g-factor [12, 13]. The solution of the corresponding eigenproblem yields the Breit-Rabi eigensystem [14]. For fields smaller than the critical field $B_c = \frac{A}{g_j\mu_B - g_p\mu_k}$ [15] the Breit-Rabi eigenstates are nearly equal to the coupled representation, whereas for larger fields the uncoupled representation is very accurate.
External electric fields, on the other hand, couple states with different orbital angular momentum L with each other, e.g. for metastable hydrogen atoms via the electric dipole interaction [12, 13]

$$H_{Stark} = e\vec{E}\cdot\vec{r}. \tag{2}$$

In case of excited atoms its impact is mainly on their lifetimes as the parity mixing goes hand in hand with coupling different long-lived states.

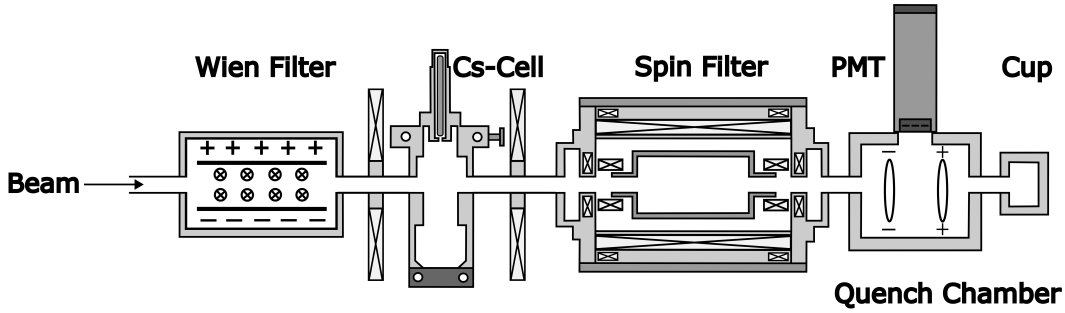

Figure 1: Sketch of the experimental set-up showing all the components of a Lamb-shift polarimeter.

3. The Lamb-shift polarimeter's working principle

The Lamb-shift polarimeter [1] is composed of several devices which are explained in detail in the following sections using an exemplary proton beam.

3.1 Wien filter

The Wien filter as the first component has several tasks to prepare the incoming proton beam for the rest of the set-up. It features a static magnetic $\vec{B}$ and a static electric field $\vec{E}$, which are perpendicular to each other as well as to the beam direction $\hat{e}_z$ such that

$$\vec{E} \perp \vec{B} \perp \vec{v}, \tag{3}$$

with $\vec{v}$ being the velocity of an incoming particle from the z-direction of the beam. Therefore, the velocity distribution of the beam is sharpened by following the next relations between the magnetic field strength B_0 and the corresponding electric field strength E_0

$$\begin{aligned} \vec{F}_{elect.} =& q\,\vec{E} = q\vec{v} \times \vec{B} = \vec{F}_{Lorentz} \\ v_0 =& \frac{E_0}{B_0}. \end{aligned} \tag{4}$$

Due to the electromagnetic repulsive forces from both fields onto the ion beam only particles with the given velocity v_0 are able to pass the device. In case of a fixed beam energy the Wien filter can also be used to separate different masses as

$$\begin{aligned} E_{Kin} &= \frac{1}{2} m v_0^2 \\ \Rightarrow \quad m &= \frac{2E_{Kin}B_0^2}{E_0^2}. \end{aligned} \tag{5}$$

Its final task is to rotate the polarization projection parallel to the beam-axis as the detection of the Lamb-shift polarimeter is sensitive to this direction only [16], which will be resolved in the subsection for the spin filter. To rotate the nuclear spin one takes advantage of the perpendicular magnetic field $\vec{B}$. As a spin interacts via its magnetic moment with external magnetic fields it

starts precessing described by the Larmor frequency. The importance in the realignment lies in the nuclear spin as its Larmor frequency ω_{Larmor} is much smaller than that of an electron

$$\omega_{Larmor} = -\frac{gqB_0}{2m}. \tag{6}$$

Here the g represents the particle's g-factor m its mass and q its charge, respectively.

3.2 Cs-cell

Once the proton beam is prepared by the Wien filter, the Cs-cell provides electrons for the protons to yield metastable hydrogen atoms. During this process it is of great importance to preserve the initial nuclear polarization. Therefore, the Cs-cell has the form of a cone, which is heated to vaporize the cesium, and it is surrounded by coils producing a holding field in beam direction up to an average value of 50 mT. The magnetic field needs to be large enough such that the electron and proton spins are uncoupled in the produced hyperfine states, which requires magnetic fields larger than the critical field $B_c = \frac{A_{2S_{1/2}}}{g_j\mu_B - g_p\mu_k} = 6.34$ mT [15]. Here $A_{2S_{1/2}}$ [17] stands for the hyperfine constants of the metastable hydrogen and g_j [12, 18] represents the Landé g-factor and g_p [19] the nuclear g-factor. Finally, $\mu_{B/k}$ stands for the Bohr- respectively the nuclear magneton. Inside the cone the incoming proton beam undergoes a charge exchange reaction leaving up to 20% of the produced hydrogen atoms in the excited metastable state [20]

$$H^+ + Cs \rightarrow H^*_{2S_{1/2}} + Cs^+. \tag{7}$$

The creation efficiency highly depends on the design of the cell and the optimal individual cell temperature.

3.3 Spin filter

The spin filter [5, 6] contains coils producing a static homogeneous magnetic field in beam direction. Inside the coils a cylindrically shaped cavity, consisting of four isolated quadrants, is connected where a radio frequency is coupled in resonance. In addition, static electric potentials are applied on two opposite quadrants of the cavity producing an electric field perpendicular to the beam axis. As explained in Sec. 2 the external fields influence the spin dynamics of the hydrogen atom. This is taken advantage of by selecting the fields so that only one Breit-Rabi state survives the time of flight through the spin filter. First, the magnetic field strength is set to produce an energy crossing between the β and e states as shown in Fig. 2. Subsequently, the static electric field couples them to quench the β states into the groundstate. Furthermore, the radio frequency, driven in the mode $TM_{0,1,0}$ [21], is used to bridge the energy gap between the crossing point and the α states to keep one of the α states trapped in an oscillation while the other one slowly decays. Therefore, the survival of the α_1 or α_2 state depends only on the corresponding magnetic field strength set to one of the two crossing points. As the two α states have different nuclear spin polarization the initial nuclear polarization of the incoming proton beam can be analyzed by ramping through the spin filter's magnetic field and comparing the corresponding signal heights with each other.

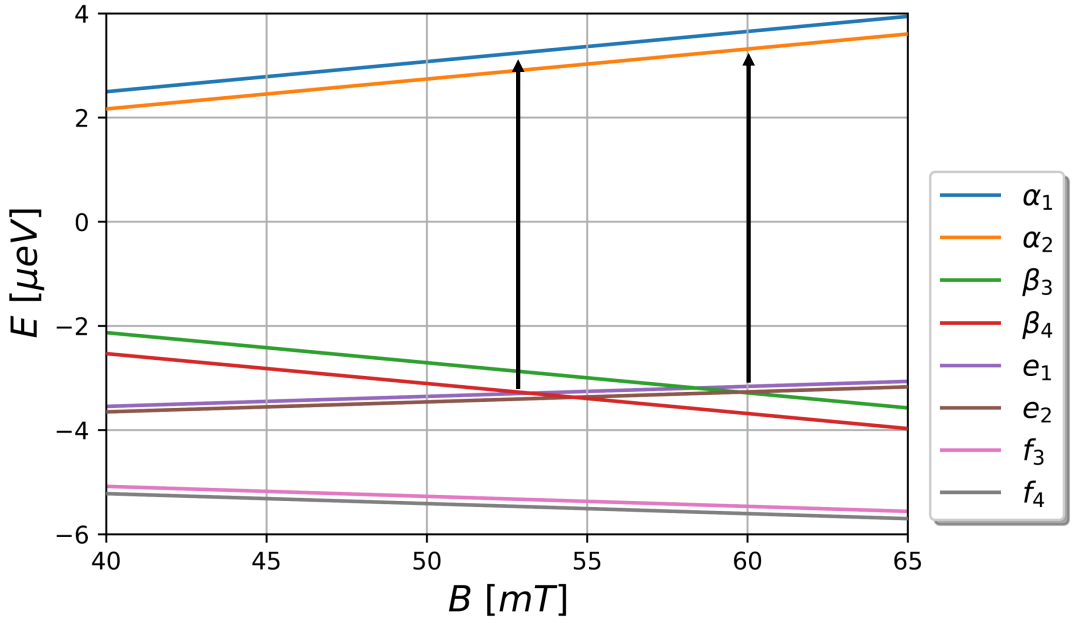

Figure 2: The Breit-Rabi diagram visualizing the energy evolution of the excited hydrogen states as function of a homogeneous external magnetic field. In addition, arrows show the reoccupation of the α states by the radio frequency.

3.4 Quenching chamber

In the quenching chamber one again takes advantage of the Stark effect [7] to quench the remaining surviving α state into the groundstate. During this process Ly-α light is emitted, which is detected by a photomultiplier [8] and converted to an electric signal displayed by an oscilloscope. As a result a relative occupation number of the α states can be observed.

4. Updated spin filter

In Sec. 3.3 the already existing spin filter is described. It features the major disadvantage that only the α states can be selected and during this process both β states are always lost. Therefore, the updated spin filter addresses this problem so that each of the four Breit-Rabi states can be transmitted individually [22]. To accomplish this task one needs to take the energetically higher $2P_{3/2}$ set into account. Correspondingly, larger magnetic field strengths are needed as the energy gap, dominated by the fine splitting, is much larger than the Lamb-shift. Nevertheless, at around 430 mT one finds again suitable energy crossings between now the α states and two states from the $2P_{3/2}$ set, as shown in Fig. 3. Therefore, a frequency of $f = 11.9$ GHz fills up the energy gap between the crossing points and the β states.

5. Automatizing process for a pulsed polarized H^- source

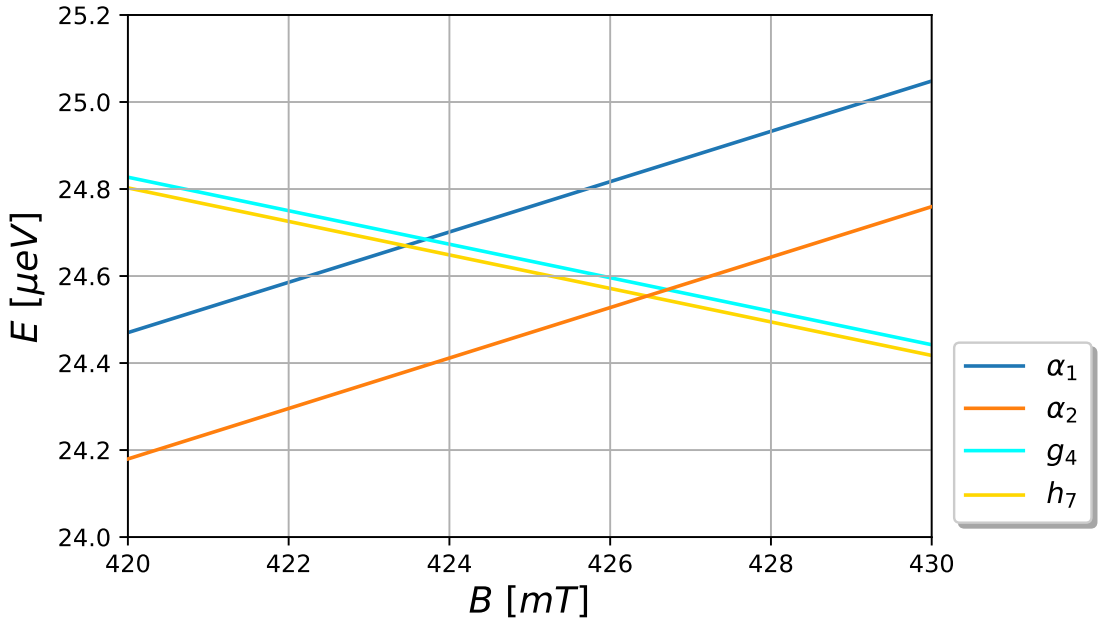

Figure 3: The figure shows the energy degeneracy between the α states with the two states (g_4, h_7) from the $2P_{3/2}$ set. For magnetic fields strong enough to decouple the magnetic moments of electron and nucleus g_4 is characterized by $m_j = -1/2$ and $m_I = -1/2$ while h_7 has $m_j = -1/2$ and $m_I = 1/2$.

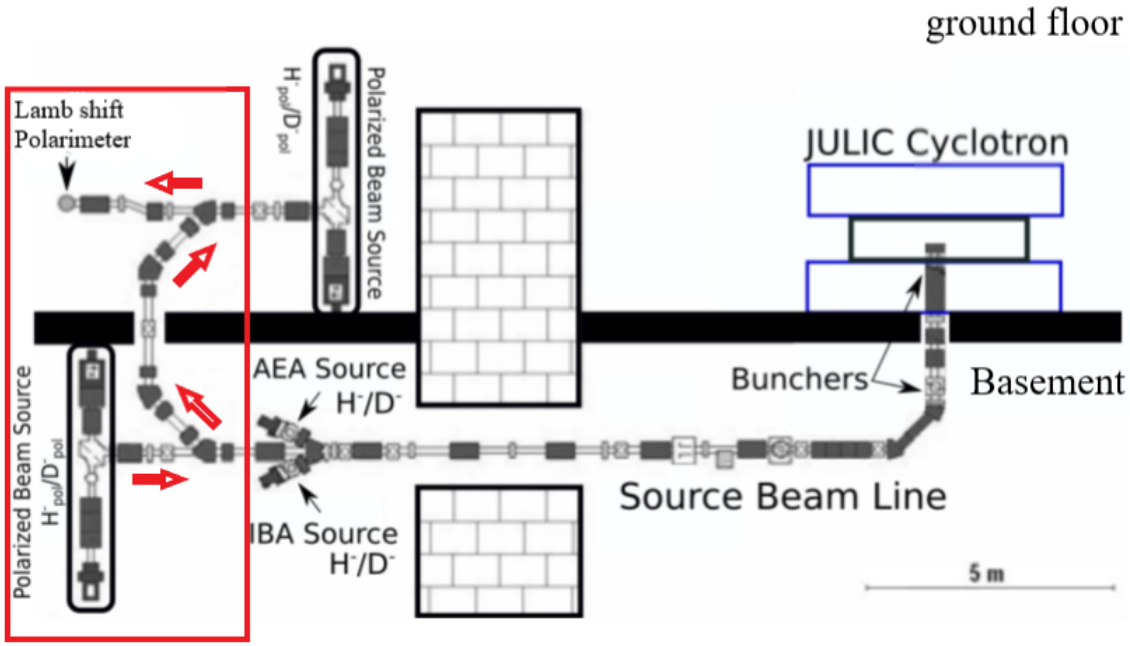

Figure 4: The picture shows the beam line from the pulsed H^- source [23] to the corresponding Lamb-shift polarimeter. Especially important is that while the polarized source is being optimized the other two sources AEA and IBA can feed the storage ring independently.

This section addresses the success of first measuring the nuclear polarization of H^- ions with a Lamb-shift polarimeter [24]. Until now the nuclear beam polarization has been measured by a low energy polarimeter (LEP) [25]. It is based on elastic nuclear scattering, i.e. the known analyzing power A_y of the C(p,p)C reaction [26, 27], which requires a cyclotron for pre-acceleration up to 45 MeV. The use of the Lamb-shift polarimeter instead, which does not need any pre-acceleration, allows for parallel operation of the unpolarized sources (IBA/AEA) to feed the COSY storage ring. In addition, it can be used to perform a live analysis to check for proper operation of a pulsed or continuous source due to an automatizing process. In Sec. 3.2, the process of generating metastable hydrogen atoms from a proton beam is described in detail. In comparison to the incoming proton beam the reaction for the H^- ions to be transformed into metastable hydrogen atoms is not yet known in detail, let alone the best temperature to achieve the most efficient metastable production rate.

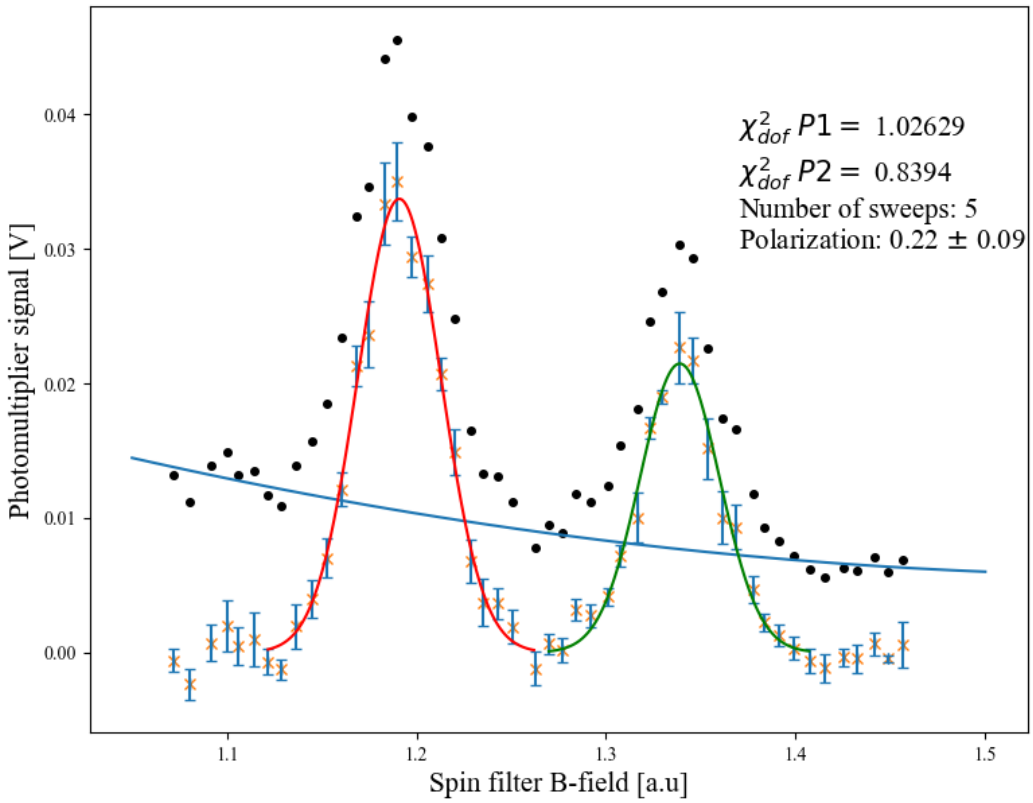

Figure 5: The signal of the photomultiplier is plotted against the magnetic field strength inside the spin filter to find the two different peaks of the α states. The black dots correspond to the mean value of the raw data. Subsequently, the orange crosses are obtained after subtracting the background. The relative height between the peaks indicates the nuclear beam polarization, here $P = 0.22 \pm 0.09$, of the pulsed H^- beam obtained after fitting with gaussian normal distributions.

6. Conclusion

To conclude, the Lamb-shift polarimeter is a simple and consistent tool to verify the nuclear and electron polarization of atoms, ions and molecules featuring hydrogen or its isotopes in a keV beam. In addition, it has been shown that an in-situ analysis for pulsed and continuous beams is possible. Moreover, the update of the spin filter makes the Lamb-shift polarimeter suitable to address new experiments with the task to determine single metastable hyperfine states of hydrogen, deuterium or tritium. In the future, the model for the updated spin filter needs to be realized. Subsequently, the optimal working condition for the Lamb-shift polarimeter for a polarized H^- source [23] needs to be determined, which will give more insight into the reaction process to produce metastable hydrogen. Finally, the similarity in the spin dynamics of $^3He^+$ ions with hydrogen gives ideas to work on a $^3He^+$ based Lamb-shift polarimeter.

7. Acknowledgement

C. Kannis acknowledges funding from the Deutsche Forschungsgemeinschaft (DFG, German Research Foundation) – 533904660.

References

[1] R. Engels, R. Emmerich, J. Ley, G. Tenckhoff, H. Paetz gen. Schieck, M. Mikirtytchiants, F. Rathmann, H. Seyfarth, and A. Vassiliev. Precision lamb-shift polarimeter for polarized atomic and ion beams. *Rev. Sci. Instrum.*, 74(11):4607–4615, 2003.

[2] W. E. Lamb and R. C. Retherford. Fine structure of the hydrogen atom by a microwave method. *Phys. Rev.*, 72:241–243, 1947.

[3] S. Klarsfeld. Radiative decay of metastable hydrogenic atoms. *Phys. Lett. A*, 30(7):382–383, 1969.

[4] W. S. Bickel and A. S. Goodman. Mean Lives of the $2p$ and $3p$ Levels in Atomic Hydrogen. *Phys. Rev.*, 148:1–4, 1966.

[5] G. Ohlsen and J. McKibben. Theory of a Radio-Frequency "Spin Filter" for a Metastable Hydrogen, Deuterium, or Tritium Atomic Beam. Technical report, Los Alamos Scientific Laboratory of the University of California, 1967.

[6] J. L. McKibben, G. P. Lawrence, and G. G. Ohlsen. Nuclear spin filter. *Phys. Rev. Lett.*, 20:1180–1182, 1968.

[7] J. Stark. Observation of the Separation of Spectral Lines by an Electric Field. *Nat.*, 92(401), 1913.

[8] ET Enterprises electron tubes, 45 Riverside Way Uxbridge UB8 2YF United Kingdom. *51 mm (2") photomultiplier 9424B series data sheet*, 2010.

[9] C. Wilkin. The legacy of the experimental hadron physics programme at COSY. *Eur. Phys. J. A*, 53(114), 2017.

[10] J. McAndrew, S. Paul, R. Emmerich, P. Fierlinger, M. Gabriel, E. Gutsmiedl, J. Mellenthin, J. Schön, W. Schott, A. Ulrich, F. Grüenauer, A. Röhrmoser, and R. Engels. Neutron bound beta-decay: BOB. *Hyperfine Interact.*, 210(1-3):13–17, 2012.

[11] R. W. Dunford and R. J. Holt. Parity violation in hydrogen revisited. *J. Phys. G: Nuclear and Particle Physics*, 34(10):2099–2118, 2007.

[12] C. Cohen-Tannoudji. *Quantum mechanics volume 2 / Claude Cohen-Tannoudji, Bernard Diu, Franck Laloe*. Wiley, 1978.

[13] H. A. Bethe and E. E. Salpeter. *Quantum Mechanics of One- and Two-Electron Atoms*. Springer Berlin, Heidelberg, 1957.

[14] G. Breit and I. I. Rabi. Measurement of nuclear spin. *Phys. Rev.*, 38:2082–2083, 1931.

[15] R. Engels. *Entwicklung eines universellen Lambshift-Polarimeters für polarisierte Atomstrahl-Targets wie an ANKE/COSY*. PhD thesis, Universität zu Köln, 2002.

[16] R. Engels, R. Gorski, K. Grigoryev, and et al. Measurement of the nuclear polarization of hydrogen and deuterium molecules using a lamb-shift polarimeter. *Rev. Sci. Instrum*, 2014.

[17] N. Kolachevsky, M. Fischer, S. G. Karshenboim, and T. W. Hänsch. High-Precision Optical Measurement of the 2*S* Hyperfine Interval in Atomic Hydrogen. *Phys. Rev. Lett.*, 92:033003, 2004.

[18] X. Fan, T. G. Myers, B. A. D. Sukra, and G. Gabrielse. Measurement of the electron magnetic moment. *Phys. Rev. Lett.*, 130:071801, 2023.

[19] C. Smorra and A. Mooser. Precision measurements of the fundamental properties of the proton and antiproton. *J. Phys. Conf. Ser.*, 1412(3):032001, 2020.

[20] B. L. Donnally, T. Clapp, W. Sawyer, and M. Schultz. Metastable hydrogen atoms produced in charge exchange. *Phys. Rev. Lett.*, 12:502–503, 1964.

[21] J. D. Jackson. *Classical electrodynamics*. New York, NY: Wiley, 2nd edition, 1975.

[22] N. Faatz, R. Engels, C. Kannis, B. Breitkreutz, and H. Soltner. Development of a complete spin filter for metastable hydrogen atoms and its isotopes. *Phys. Open*, 22:100248, 2025.

[23] R. Weidmann, A. Glombik, H. Meyer, W. Kretschmer, M. Altmeier, P. D. Eversheim, O. Felden, R. Gebel, M. Glende, M. Eggert, S. Lemaitre, R. Reckenfelderbäumer, and H. Paetz gen. Schieck. The polarized ion source for COSY. *Rev. Sci. Instrum.*, 67(3):1357–1358, 1996.

[24] S. J. Pütz. Polarization measurements of a H^- ion beam. Master thesis, University of Cologne, 2024.

[25] C. Zheng, R. Engels, C. Kannis, O. Felden, A. Lehrach, and M. Büscher. Tests of a polarimeter for laser-driven proton beams at the 45-MeV cyclotron JULIC. *PoS*, PSTP2022:031, 2023.

[26] Y. Tagishi, N. Nakamoto, K. Katoh, J. Togawa, T. Hisamune, T. Yoshida, and Y. Aoki. Analyzing powers for ^{2}H(d,p)^{3}H at incident energies of 30, 50, 70, and 90 keV. *Phys. Rev. C*, 46:R1155–R1158, 1992.

[27] B. Becker, R. Randermann, B. Polke, S. Lemaître, R. Reckenfelderbäumer, P. Niessen, G. Rauprich, L. Sydow, and H. P. Schieck. Measurement of a complete set of analyzing powers of the fusion reactions D($\vec{d}$,p)^{3}He at E_d=28 keV. *Few-Body Syst.*, 13:19–39, 1992.